

PAPER

An Efficient Channel Estimation Scheme Using Walsh Pilots in Bi-directional Wireless OFDM Relay Systems with Analog Network Coding

Yuta KOSHIMIZU^{†a)} and Eiji OKAMOTO[†], *Members*

SUMMARY In this paper, we propose an efficient channel estimation scheme in bi-directional wireless orthogonal frequency division multiplexing (OFDM) relay systems applying analog network coding (ANC). In the relay systems applying ANC, channel separation is needed to estimate each of the bi-directional channels simultaneously from the combined received signal. In the conventional channel estimation schemes, relatively higher-ratio pilots are needed to obtain accurate channels. In contrast, we propose a channel estimation scheme with sparse pilots, while maintaining high accuracy for channel estimation. In the proposed scheme, Walsh codes are inserted as the pilot symbols at both end nodes, and the individual channels are obtained by correlation processing from the combined signals. The improved bit error rate (BER) and throughput performances of the proposed scheme are shown through computer simulations.

key words: channel estimation, OFDM, analog network coding, Walsh code

1. Introduction

A transmission technique in which the transmit and receive nodes communicate with each other through the relay nodes is known as a relay system. Relay systems produce many benefits in flexible network formation and the expansion of communication areas. However, in bi-directional relay systems, throughput degradation occurs owing to the requirement of many time slots to avoid interference in bi-directional transmission at the relay node. To address this problem, network coding (NC) techniques [1]–[4] have been proposed, which can be roughly divided into digital network coding (DNC) [1], [2] and analog network coding (ANC) [3], [4]. The Alice and Bob topology, in which two transmit/receive nodes communicate with each other through one relay node, as shown in Fig. 1(a), is considered in this study as a bi-directional relay system. In the Alice and Bob topology, bi-directional transmission without NC needs four time slots, as shown in Fig. 1(b), and DNC needs three time slots, as shown in Fig. 1(c), but ANC can terminate the transmission with only two time slots, as shown in Fig. 1(d). This means that the ANC scheme can double the throughput as compared with a non-NC scheme and increase the throughput 1.5 times as compared with the DNC scheme. The ANC scheme is particularly effective in wireless communication,

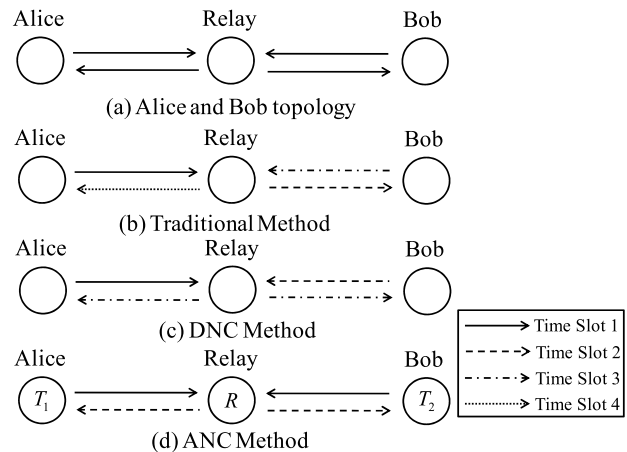


Fig. 1 Bi-directional relay in Alice and Bob topology.

as the frequency resources are limited. In wireless communications, because the channel state is changed, the channel estimation and equalization for all links at each time slot are needed. However, in the ANC scheme, the relay node receives the combined signals from both end nodes at Time Slot 1, as shown in Fig. 1(d). Thus, channel separation is needed to estimate each of the channels. Some channel separation and estimation schemes in the bi-directional relay with ANC have been proposed in [5], [6]. In both [5] and [6], interference in the superimposed signal is avoided by using phase-shifted pilots between both end nodes and by orthogonalizing the channels. In [5], channel estimation is carried out at each time slot, whereas in [6], channel estimation is jointly carried out at Time Slot 2 in Fig. 1(d). In contrast to [5], channel feedback from the relay node is not necessary in [6]. It is concluded that the throughput performance can be improved by omitting the channel feedback from the relay to the end nodes while the degradation of channel estimation accuracy is restricted. However, in [5], [6], one entire orthogonal frequency division multiplexing (OFDM) frame is needed as the pilot to estimate the channel, as shown in Fig. 2(a), which is called “block type” hereafter. This frame structure decreases the rate efficiency. To address this problem, we have proposed channel estimation schemes with sparse pilots, as shown in Fig. 2(b) [7], [8]. The proposed schemes use Walsh codes as pilots [9], [10], and the channels are separated by correlation pro-

Manuscript received November 1, 2012.

Manuscript revised March 11, 2013.

[†]The authors are with the Department of Computer Science and Engineering, Graduate School of Engineering, Nagoya Institute of Technology, Nagoya-shi, 466-8555 Japan.

a) E-mail: 23417554@stn.nitech.ac.jp

DOI: 10.1587/transcom.E96.B.2119

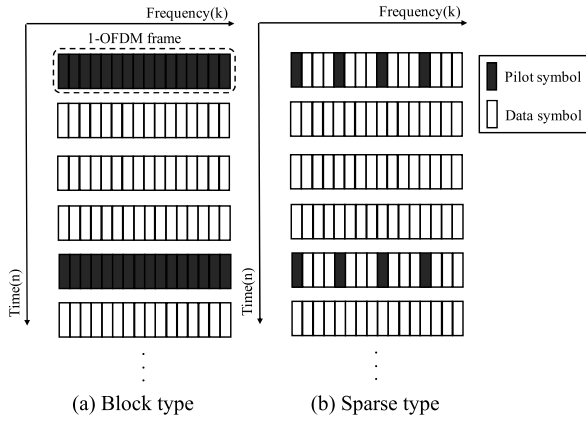


Fig. 2 Pilot frame structures.

cessing based on Walsh code orthogonality at the receiver. Correlation processing of the proposed schemes is obtained by the extension of conventional correlation processing [10] and is more robust to time-selective fading. The scheme of [7] estimates channels at each time slot, whereas the scheme of [8] estimates channels only at Time Slot 2. We have confirmed in [8] that throughput improvement is achieved by the skip in channel feedback, similar to [5], [6]. However, in [7], [8], channel coding was not considered. Usually, channel coding is indispensable in improving the performance of wireless communication systems. Therefore, in this paper, we propose an efficient channel estimation scheme using sparse Walsh pilots in bi-directional ANC-based wireless OFDM relay systems while considering channel coding and show the improved performances.

The remainder of this paper is organized as follows. The bi-directional network model is described in Sect. 2. The classification of channel estimation and the proposed schemes are introduced in Sect. 3. Additionally, the two-dimensional fast Fourier transform (FFT)-based interpolation scheme is introduced in Sect. 3. In Sect. 4, numerical results are shown, and the conclusions are drawn in Sect. 5.

2. System Model

The system model considered in this paper is a bi-directional two-time slot wireless OFDM relay system with ANC, as shown in Fig. 1(d). Nodes T_1 and T_2 communicate with each other through relay node R , as they cannot communicate directly. Each node equips one antenna, and the channel is half duplex. We assume a time and frequency selective fading channel as each node moves.

In Time Slot 1, nodes T_1 and T_2 send their data to relay node R . Let $S_i(k)$ ($k = 0, \dots, N-1$) be the frequency-domain transmit symbol of node T_i ($i = 1, 2$) after the first modulation at subcarrier k , where N is the number of subcarriers. The N -symbol time sequence of OFDM is obtained by an N -point inverse fast Fourier transform (IFFT) of $S_i(k)$ at each T_i . After the addition of N_{GI} symbol guard intervals (GI), the composed OFDM time sequence is transmitted to relay node R . The received symbol $R_{1,r}(k)$ at relay node R

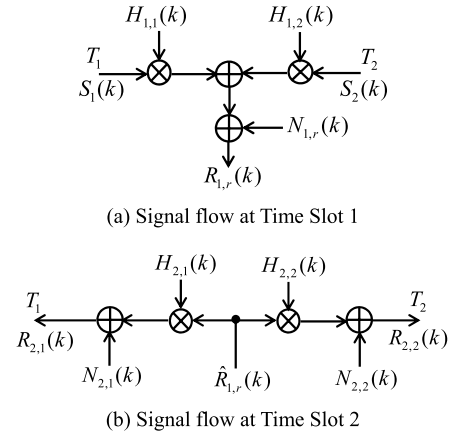


Fig. 3 Frequency-domain block diagram of bi-directional transmission at each time slot.

after removal of the GI and FFT is described by

$$R_{1,r}(k) = \sum_{i=1}^2 H_{1,i}(k) S_i(k) + N_{1,r}(k) \quad (k = 0, \dots, N-1) \quad (1)$$

where $H_{1,i}(k)$ is the frequency-domain channel coefficient between node T_i and relay R , and $N_{1,r}(k)$ is a zero-mean Gaussian noise in relay R at Time Slot 1. The transmitter and receiver block diagram at Time Slot 1 is shown in Fig. 3(a). In this figure, Time Slot 1 can be regarded as a multiple-input single-output (MISO) transmission.

In Time Slot 2, the relay node R normalizes the received signal $R_{1,r}(k)$ to generate a forwarding signal $\hat{R}_{1,r}(k)$ as follows:

$$\begin{aligned} \hat{R}_{1,r}(k) &= G R_{1,r}(k) \quad (k = 0, \dots, N-1), \\ G &= 1 / \sqrt{E \{ |R_{1,r}(k)|^2 \}} \end{aligned} \quad (2)$$

where G is the normalization gain factor, and $E\{\cdot\}$ is an expectation value, and thus, the average transmit power is normalized to 1. $\hat{R}_{1,r}(k)$ is transmitted to each node T_i after the IFFT and GI insertion. As shown in Fig. 3(b), the received symbol $R_{2,i}(k)$ at node T_i after GI removal and the FFT is described by

$$R_{2,i}(k) = H_{2,i}(k) \hat{R}_{1,r}(k) + N_{2,i}(k) \quad (k = 0, \dots, N-1) \quad (3)$$

where $H_{2,i}(k)$ and $N_{2,i}(k)$ are the channel coefficient between relay R and node T_i and zero-mean Gaussian noise at node T_i , respectively. Time Slot 2 can be regarded as two parallel single-input single-output (SISO) transmissions. The received signal $R_{2,i}(k)$ contains the transmit data of both nodes T_1 and T_2 , and thus, each node has to subtract its own transmit data before decoding. This subtraction is given by

$$\begin{aligned} \hat{R}_{2,i}(k) &= R_{2,i}(k)/G - H_{1,i}(k) H_{2,i}(k) S_i(k) \\ &\quad (k = 0, \dots, N-1) \quad (i = 1, 2) \end{aligned} \quad (4)$$

Then, the transmit data of the opposite node $\hat{S}_j(k)$ is obtained by equalization of $\hat{R}_{2,i}(k)$ as follows:

$$\hat{S}_j(k) = \frac{\hat{R}_{2,i}(k)}{H_{1,j}(k)H_{2,i}(k)} \quad (k=0, \dots, N-1) \quad (j=2, 1) \quad (5)$$

Here, Eq. (5) is the zero-forcing (ZF) equalization, and j is calculated by

$$j = (3 - i) = \begin{cases} 1 & \text{if } i = 2 \\ 2 & \text{if } i = 1 \end{cases} \quad (6)$$

After the calculation of Eq. (5) at nodes T_1 and T_2 , the bi-directional relay transmission is terminated.

From Eqs. (4)–(6), in the bi-directional relay systems with ANC, node T_i at Time Slot 2 needs combined channel coefficient $H_{1,i}(k)H_{2,i}(k)$ for self-data subtraction and $H_{1,j}(k)H_{2,i}(k)$ for equalization. The channel estimation schemes for these channel coefficients are proposed in Sect. 3.

3. Channel Estimation

3.1 Two Architectures of Channel Estimation Classified by Estimation Node Location

The channel estimation (CE) schemes in bi-directional OFDM relay systems with ANC are classified into two types by the estimation node location [5], [6].

In the first scheme, relay R estimates the channel coefficients $H_{1,1}(k)$ and $H_{1,2}(k)$ in Time Slot 1, and node T_i estimates the channel coefficient $H_{2,i}(k)$ in Time Slot 2. In this scheme, channel separation is required at relay R , and the channel feedback from relay R to T_i is also required. When the channel coefficients are fed back, node T_i knows $H_{1,1}(k)$, $H_{1,2}(k)$, and $H_{2,i}(k)$, and it calculates the combined coefficient $H_{1,i}(k)H_{2,i}(k)$ for self-data subtraction given by Eq. (4) and $H_{1,(3-i)}(k)H_{2,i}(k)$ for equalization given by Eq. (5). This scheme requires channel feedback and is labeled as “CE with feedback” hereafter. The drawback of this scheme is throughput degradation due to feedback.

In the second scheme, node T_i at Time Slot 2 estimates the combined channel coefficients $H_{1,i}(k)H_{2,i}(k)$ for self-data subtraction and $H_{1,(3-i)}(k)H_{2,i}(k)$ for equalization. In contrast to the feedback scheme, channel separation originating from the overlapped reception in Time Slot 1 shown in Fig. 3(a) is needed at node T_i . However, channel feedback can be omitted. Thus, we label this scheme as the channel estimation scheme without feedback (CE without feedback). The drawback of this scheme is that it leads to the degradation of channel estimation accuracy as the pilots at node T_i in Time Slot 2 contain Gaussian noise equivalent to two time slots.

3.2 Three Architectures of Channel Estimation Classified by Pilot-Symbol Assignment

Channel separation is needed in both CE with feedback and CE without feedback. It is achieved by the pilot symbol assignment such that two channels are orthogonally divided. In this study, we classify the pilot frame structure into three

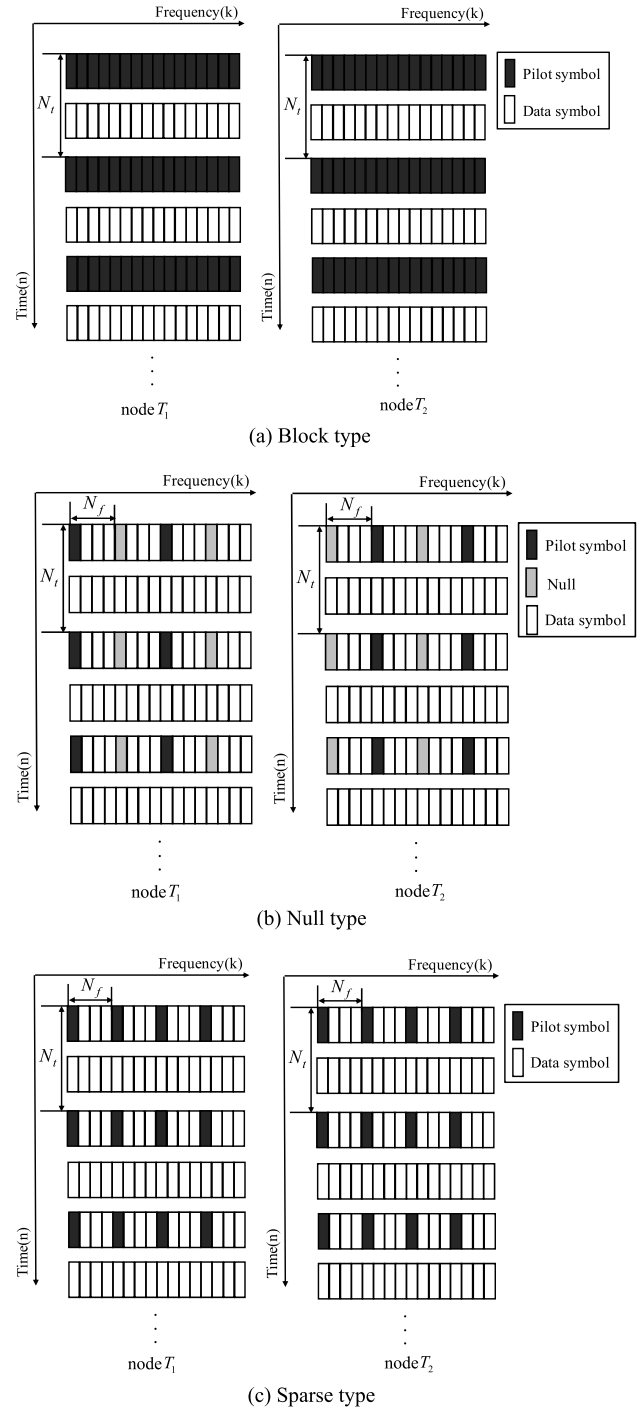


Fig. 4 Pilot-symbol design for channel separation in bi-directional transmission.

types.

The first pilot frame is shown in Fig. 4(a), where the pilots are inserted as one entire OFDM frame. This frame structure is called “block type.” The CE with feedback adopting a block-type frame structure is proposed in [5], and the CE without feedback adopting this type is proposed in [6]. Both schemes separate the channel coefficients from the overlapped signals and achieve high-accuracy channel esti-

mation. However, the block-type frame needs a relatively higher ratio of pilots.

The second pilot frame is shown in Fig. 4(b), where pilot symbols and null are alternately assigned [11], and this structure is called “null type” hereafter. The received pilot symbols at the relay node can be orthogonal because the null insertion and channel separation are not needed. As compared with the block-type frame, the null type can reduce the pilot ratio. However, because the interval of pilots for each node doubles because of the null insertion, relatively dense pilots will be needed to enhance the channel accuracy.

The third pilot frame, called “sparse type,” is shown in Fig. 4(c). Sparse pilots in the time and frequency directions are assigned at the same pattern, and some separation methods are used at the relay or end nodes. This type can reduce the pilot ratio as compared with that shown in Fig. 4(a) and can also obtain a short pilot interval as compared with that shown in Fig. 4(b), so that the throughput performance is improved. In this paper, the sparse-type frame is taken into consideration.

3.3 Proposed Channel Estimation Scheme with Feedback

The signal processing of each time slot is based on the scheme of [5]. In what follows, the proposed channel estimation scheme is described.

3.3.1 Channel Estimation in Time Slot 1

In the proposed scheme, Walsh codes are used as pilot symbols to achieve channel estimation with the sparse-type frame. We use a 2-by-2 Walsh code, as shown below, as the pilots:

$$\mathbf{W}_2 = \begin{bmatrix} w_{11} & w_{12} \\ w_{21} & w_{22} \end{bmatrix} = \begin{bmatrix} 1 & 1 \\ 1 & -1 \end{bmatrix} \quad (7)$$

where column 1 is assigned to node T_1 , and column 2 is assigned to node T_2 . Walsh pilot $P_{1,i}(k, n)$ of node T_i is described by

$$P_{1,i}(k, n) = w_{xi}, \quad x = \text{mod}(n/N_t, 2) + 1 \\ (k = 0, N_f, 2N_f, \dots), (n = 0, N_t, 2N_t, \dots) \quad (8)$$

where k and n are the frequency and time indices, respectively, $\text{mod}(a, b)$ is the remainder of a divided by b , and N_f and N_t are the period of the Walsh pilot symbol in the frequency and the time domains, respectively. The frame structure using Walsh pilots based on Eq. (8) is shown in Fig. 5. These Walsh pilots enable the orthogonal separation of channel coefficients T_1 and T_2 after correlation processing at relay node R .

First, we explain the correlation processing in [10] as conventional correlation processing. The received symbol $R_{1,r}(k, n)$ at relay node R can be written as

$$R_{1,r}(k, n) = \sum_{i=1}^2 H_{1,i}(k, n) P_{1,i}(k, n) + N_{1,r}(k, n) \\ (k = 0, N_f, 2N_f, \dots), (n = 0, N_t, 2N_t, \dots) \quad (9)$$

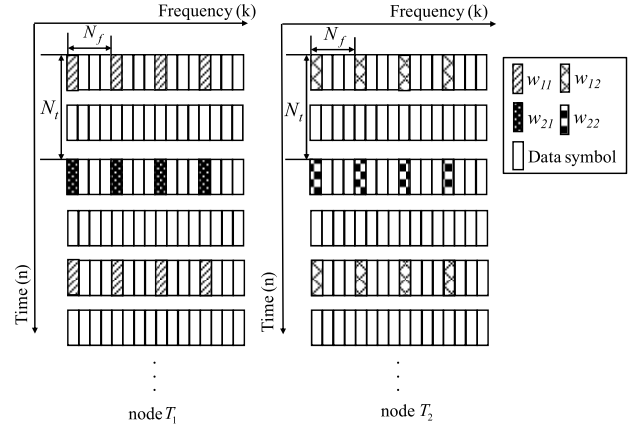


Fig. 5 Proposed pilot frame in Time Slot 1.

where the subcarriers of Walsh pilots on the pilot frame are only considered. The received signals $R_{1,r}(k, n)$ are overlapped signals from node T_1 and node T_2 , and the relay node R separates the channel between node T_i and R described by $\hat{H}_{1,i}^{con.}(k, n)$ from $R_{1,r}(k, n)$ by correlation processing based on Walsh code orthogonality, which is given by

$$\hat{H}_{1,i}^{con.}(k, n) = \frac{1}{2} \sum_{l=-1}^0 R_{1,r}(k, n + lN_t) P_{1,i}(k, n + lN_t) \\ (k = 0, N_f, 2N_f, \dots), (n = 0, N_t, 2N_t, \dots) \quad (10)$$

Here, we confirm the extraction of $\hat{H}_{1,1}^{con.}(k, n)$ from $R_{1,r}(k, n)$ using Eq. (10) when $\text{mod}(n/N_t, 2) = 0$ as an example. Equation (10) is expanded as follows

$$\hat{H}_{1,1}^{con.}(k, n) = \frac{1}{2} (H_{1,1}(k, n - N_t) + H_{1,1}(k, n)) \\ + \frac{1}{2} (-H_{1,2}(k, n - N_t) + H_{1,2}(k, n)) \\ + \frac{1}{2} (N_{1,r}(k, n - N_t) + N_{1,r}(k, n)) \\ = H_{1,1}(k, n) + \Delta_1^{w.con.} + \Delta_2^{w.con.} + \Delta_3^{w.con.} \quad (11)$$

where the interference terms are given by

$$\begin{cases} \Delta_1^{w.con.} = \frac{1}{2} (-H_{1,1}(k, n - N_t) + H_{1,1}(k, n)) \\ \Delta_2^{w.con.} = \frac{1}{2} (-H_{1,2}(k, n - N_t) + H_{1,2}(k, n)) \\ \Delta_3^{w.con.} = \frac{1}{2} (N_{1,r}(k, n - N_t) + N_{1,r}(k, n)) \end{cases} \quad (12)$$

In the conventional correlation processing, three interference terms occur along with objective channel coefficient $H_{1,1}(k, n)$. $\Delta_1^{w.con.}$ and $\Delta_2^{w.con.}$ are the interferences due to the time variance of the channel, and $\Delta_3^{w.con.}$ is the Gaussian noise. Interferences $\Delta_1^{w.con.}$ and $\Delta_2^{w.con.}$ become asymptotical to zero when the channel coefficient $H_{1,1}(k, n)$ is static or the interval of the Walsh pilot symbol in the time direction N_t is small. However, when the channel is dynamic, or N_t is large, $\Delta_1^{w.con.}$ and $\Delta_2^{w.con.}$ become large and the channel estimation accuracy is degraded. In contrast, because the two independent terms in $\Delta_3^{w.con.}$ are averaged, the Gaussian

noise is mitigated.

Next, we propose an improved correlation processing method. In the proposed correlation processing method, the channel coefficient $\hat{H}_{1,i}^{pro.}(k, n)$ is estimated with more pilots to suppress the degradation of channel estimation as follows:

$$\hat{H}_{1,i}^{pro.}(k, n) = \frac{1}{2} \left(\frac{1}{2} \sum_{l=-1}^0 R_{1,r}(k, n + lN_t) P_{1,i}(k, n + lN_t) + \frac{1}{2} \sum_{l=0}^1 R_{1,r}(k, n + lN_t) P_{1,i}(k, n + lN_t) \right) \quad (k=0, N_f, 2N_f, \dots), (n=0, N_t, 2N_t, \dots) \quad (13)$$

Here, we confirm the extraction of $\hat{H}_{1,i}^{pro.}(k, n)$ from $R_{1,r}(k, n)$ using Eq. (13) when $\text{mod}(n/N_t, 2) = 0$ as an example. Equation (13) can be expanded as follows:

$$\begin{aligned} \hat{H}_{1,i}^{pro.}(k, n) &= \frac{1}{4} (H_{1,1}(k, n - N_t) + 2H_{1,1}(k, n) + H_{1,1}(k, n + N_t)) \\ &\quad + \frac{1}{4} (-H_{1,2}(k, n - N_t) + 2H_{1,2}(k, n) - H_{1,2}(k, n + N_t)) \\ &\quad + \frac{1}{4} (N_{1,r}(k, n - N_t) + 2N_{1,r}(k, n) + N_{1,r}(k, n + N_t)) \\ &= H_{1,1}(k, n) + \Delta_1^{w.pro.} + \Delta_2^{w.pro.} + \Delta_3^{w.pro.} \end{aligned} \quad (14)$$

where the interference terms are

$$\begin{cases} \Delta_1^{w.pro.} = \frac{1}{4} (H_{1,1}(k, n - N_t) - 2H_{1,1}(k, n) + H_{1,1}(k, n + N_t)) \\ \Delta_2^{w.pro.} = \frac{1}{4} (-H_{1,2}(k, n - N_t) + 2H_{1,2}(k, n) - H_{1,2}(k, n + N_t)) \\ \Delta_3^{w.pro.} = \frac{1}{4} (N_{1,r}(k, n - N_t) + 2N_{1,r}(k, n) + N_{1,r}(k, n + N_t)) \end{cases} \quad (15)$$

In the proposed correlation processing, the three interference terms occur along with objective channel coefficient $H_{1,1}(k, n)$, the same as in Eq. (11). However, in the proposed correlation processing, $\Delta_1^{w.pro.}$ and $\Delta_2^{w.pro.}$ become nearly zero not only when the channel coefficient $H_{1,1}(k, n)$ is static, or the pilot interval in the time direction (N_t) is small, but also when the channel coefficient $H_{1,1}(k, n)$ changes linearly in the period of $[n - N_t, n + N_t]$. This means that the proposed correlation processing is robust against the time-selective fading. Furthermore, because three independent terms in $\Delta_3^{w.pro.}$ are averaged, Gaussian noise is further mitigated.

3.3.2 Channel Estimation in Time Slot 2

The relay node R in Time Slot 2, which conducts two parallel SISO transmissions to both nodes T_i , replaces the pilot symbols from Time Slot 1. Pilot symbols $P_2(k, n)$ at the relay node R are given by

$$P_2(k, n) = \text{pilot}(k, n) \quad (k = 0, N'_f, 2N'_f, \dots), (n = 0, N'_t, 2N'_t, \dots) \quad (16)$$

where $\text{pilot}(k, n)$ is a pilot symbol such as 1, and N'_f and N'_t are the periods of the pilot symbol in the frequency and the time domains, respectively. The frame structure in Time Slot 2 is shown in Fig. 6. The received symbol $R_{2,i}(k, n)$ at node T_i in the frequency domain is obtained by

$$R_{2,i}(k, n) = H_{2,i}(k, n)P_2(k, n) + N_{2,i}(k, n) \quad (k = 0, N'_f, 2N'_f, \dots), (n = 0, N'_t, 2N'_t, \dots) \quad (17)$$

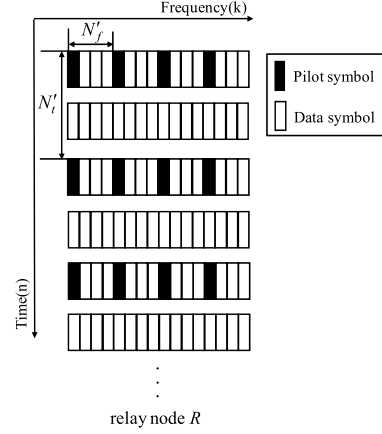


Fig. 6 Proposed pilot frame in Time Slot 2.

where only the subcarriers of the pilot symbols in the pilot frame are considered. At node T_i , the estimated channel $\hat{H}_{2,i}(k, n)$ is obtained from the received signal $R_{2,i}(k, n)$ as follows:

$$\hat{H}_{2,i}(k, n) = \frac{R_{2,i}(k, n)}{P_2(k, n)} = H_{2,i}(k, n) + \frac{N_{2,i}(k, n)}{P_2(k, n)} \quad (k = 0, N'_f, 2N'_f, \dots), (n = 0, N'_t, 2N'_t, \dots) \quad (18)$$

Using these calculated channel coefficients at the pilots, the channel coefficients at data symbols are interpolated (described in Sect. 3.5). Finally, node T_i subtracts the self-data and equalizes using estimated channel $\hat{H}_{2,i}(k, n)$ and fed back channel $\hat{H}_{1,i}(k, n)$ from relay node R , as described in Eqs. (4) and (5). Then, the transmitted data are obtained.

3.4 Proposed Channel Estimation Scheme without Feedback

In the channel estimation scheme without feedback, the relay node R in Time Slot 1 does not estimate the channels, and node T_i estimates the desired channels at once in Time Slot 2. The pilot frame structure at node T_i in Time Slot 1 is identical with Eq. (8), and the received symbol at the relay node R is identical with Eq. (9). In contrast to Sect. 3.3, the channel estimation scheme without feedback does not estimate channels in Time Slot 1, and Walsh pilots are simply broadcasted to node T_i after normalization with amplification factor G . The received pilot symbol $R_{2,i}(k, n)$ at node T_i in the frequency domain and Time Slot 2 is obtained by

$$R_{2,i}(k, n) = GR_{1,r}(k, n)H_{2,i}(k, n) + N_{2,i}(k, n) \quad (k = 0, N'_f, 2N'_f, \dots), (n = 0, N'_t, 2N'_t, \dots) \quad (19)$$

Because the received symbol $R_{2,i}(k, n)$ contains the channel coefficients of both nodes T_1 and T_2 , node T_i separates and estimates the channels for self-data subtraction and equalization of Eqs. (4)–(6) by correlation processing.

Similar to Sect. 3.3.1, we first explain the correlation processing adopted in [10] as the conventional correlation processing. Node T_i calculates the channel coefficient $\hat{H}_{1,i}^{con.}(k, n)\hat{H}_{2,i}^{con.}(k, n)$ for self-data subtraction and

channel coefficient $\hat{H}_{1,(3-i)}^{con.}(k, n)\hat{H}_{2,i}^{con.}(k, n)$ for equalization as follows:

$$\hat{H}_{1,s}^{con.}(k, n)\hat{H}_{2,i}^{con.}(k, n) = \frac{1}{2G} \sum_{l=-1}^0 R_{2,i}(k, n + lN_t)P_{1,s}(k, n + lN_t) \quad (k = 0, N_f, 2N_f, \dots), (n = 0, N_t, 2N_t, \dots) \quad (20)$$

where $s = i$ for self-data subtraction, and $s = 3 - i$ for equalization. Here, we confirm the extraction of $\hat{H}_{1,1}^{con.}(k, n)\hat{H}_{2,1}^{con.}(k, n)$ from $R_{2,1}(k, n)$ using Eq. (20) when $\text{mod}(n/N_t, 2) = 0$, as an example. Equation (20) is expanded as follows:

$$\begin{aligned} & \hat{H}_{1,1}^{con.}(k, n)\hat{H}_{2,1}^{con.}(k, n) \\ &= \frac{1}{2G} \sum_{l=-1}^0 R_{2,1}(k, n + lN_t)P_{1,1}(k, n + lN_t) \\ &= H_{1,1}(k, n)H_{2,1}(k, n) + \Delta_1^{wo.con.} + \Delta_2^{wo.con.} + \Delta_3^{wo.con.} \end{aligned} \quad (21)$$

where

$$\begin{cases} \Delta_1^{wo.con.} = \frac{1}{2}(-H_{1,1}(k, n - N_t)H_{2,1}(k, n - N_t) \\ \quad + H_{1,1}(k, n)H_{2,1}(k, n)) \\ \Delta_2^{wo.con.} = \frac{1}{2}(-H_{1,2}(k, n - N_t)H_{2,1}(k, n - N_t) \\ \quad + H_{1,2}(k, n)H_{2,1}(k, n)) \\ \Delta_3^{wo.con.} = \frac{1}{2G} \left(GN_{1,r}(k, n - N_t)H_{2,1}(k, n - N_t) + N_{2,1}(k, n - N_t) \right) \\ \quad + GN_{1,r}(k, n)H_{2,1}(k, n) + N_{2,1}(k, n) \end{cases} \quad (22)$$

$\Delta_1^{wo.con.}$ and $\Delta_2^{wo.con.}$ are the interferences due to the time variance of the combined channel, and $\Delta_3^{wo.con.}$ is the Gaussian noise as well as Sect. 3.3. However, the elements of $\Delta_1^{wo.con.}$ and $\Delta_2^{wo.con.}$ contain a channel coefficient $H_{2,1}(k, n)$ as compared to $\Delta_1^{w.con.}$ and $\Delta_2^{w.con.}$ in Eq. (12). In addition, $\Delta_3^{wo.con.}$ has more elements than $\Delta_3^{w.con.}$. Interferences $\Delta_1^{wo.con.}$ and $\Delta_2^{wo.con.}$ become asymptotical to zero when the combined channel is static, or N_t is small. However, when the channel is dynamic, or N_t is large, $\Delta_1^{wo.con.}$ and $\Delta_2^{wo.con.}$ become large and degrade the channel estimation accuracy. However, because $\Delta_3^{wo.con.}$ has more elements than $\Delta_3^{w.con.}$, $\Delta_3^{wo.con.}$ is mitigated by the arithmetic average.

Next, we explain the proposed correlation processing. Node T_i calculates the channel coefficient $\hat{H}_{1,i}^{pro.}(k, n)\hat{H}_{2,i}^{pro.}(k, n)$ for self-data subtraction and the channel coefficient $\hat{H}_{1,(3-i)}^{pro.}(k, n)\hat{H}_{2,i}^{pro.}(k, n)$ for equalization using more pilots to suppress the degradation as follows:

$$\begin{aligned} & \hat{H}_{1,s}^{pro.}(k, n)\hat{H}_{2,i}^{pro.}(k, n) \\ &= \frac{1}{2G} \left(\frac{1}{2} \sum_{l=-1}^0 R_{2,i}(k, n + lN_t)P_{1,s}(k, n + lN_t) \right. \\ & \quad \left. + \frac{1}{2} \sum_{l=0}^1 R_{2,i}(k, n + lN_t)P_{1,s}(k, n + lN_t) \right) \quad (k = 0, N_f, 2N_f, \dots), (n = 0, N_t, 2N_t, \dots) \end{aligned} \quad (23)$$

where $s = i$ for self-data subtraction, and $s = 3 - i$ for equalization. Here, as an example, we confirm the extraction of $\hat{H}_{1,1}^{pro.}(k, n)\hat{H}_{2,1}^{pro.}(k, n)$ from $R_{2,1}(k, n)$ using Eq. (23) when $\text{mod}(n/N_t, 2) = 0$. Equation (23) is expanded as follows:

$$\begin{aligned} & \hat{H}_{1,1}^{pro.}(k, n)\hat{H}_{2,1}^{pro.}(k, n) \\ &= \frac{1}{2G} \left(\frac{1}{2} \sum_{l=-1}^0 R_{2,1}(k, n + lN_t)P_{1,1}(k, n + lN_t) \right. \\ & \quad \left. + \frac{1}{2} \sum_{l=0}^1 R_{2,1}(k, n + lN_t)P_{1,1}(k, n + lN_t) \right) \\ &= H_{1,1}(k, n)H_{2,1}(k, n) + \Delta_1^{wo.pro.} + \Delta_2^{wo.pro.} + \Delta_3^{wo.pro.} \end{aligned} \quad (24)$$

where

$$\begin{cases} \Delta_1^{wo.pro.} = \frac{1}{4} \left(H_{1,1}(k, n - N_t)H_{2,1}(k, n - N_t) \right. \\ \quad \left. - 2H_{1,1}(k, n)H_{2,1}(k, n) \right. \\ \quad \left. + H_{1,1}(k, n + N_t)H_{2,1}(k, n + N_t) \right) \\ \Delta_2^{wo.pro.} = \frac{1}{4} \left(-H_{1,2}(k, n - N_t)H_{2,1}(k, n - N_t) \right. \\ \quad \left. + 2H_{1,2}(k, n)H_{2,1}(k, n) \right. \\ \quad \left. - H_{1,2}(k, n + N_t)H_{2,1}(k, n + N_t) \right) \\ \Delta_3^{wo.pro.} = \frac{1}{4G} \left(GN_{1,r}(k, n - N_t)H_{2,1}(k, n - N_t) \right. \\ \quad \left. + N_{2,1}(k, n - N_t) \right. \\ \quad \left. + 2GN_{1,r}(k, n)H_{2,1}(k, n) + 2N_{2,1}(k, n) \right. \\ \quad \left. + GN_{1,r}(k, n + N_t)H_{2,1}(k, n + N_t) \right. \\ \quad \left. + N_{2,1}(k, n + N_t) \right) \end{cases} \quad (25)$$

Similar to Sect. 3.3.1, in the proposed correlation processing, the interference is more mitigated than in the conventional processing. Furthermore, because the number of elements of $\Delta_3^{wo.pro.}$ is greater than $\Delta_3^{wo.con.}$, the Gaussian noise is further mitigated.

3.5 Pilot Interpolation using Two-Dimensional FFT

In Sects. 3.3 and 3.4, we proposed the channel estimation scheme in the pilot subcarriers. In the fading channel, an accurate interpolation should be applied to obtain the channel coefficients in all data subcarriers. In this paper, because we adopt the pilot frame in which pilots are assigned sparsely in the frequency and the time domains, two-dimensional interpolation should be applied. To achieve the channel estimation for all subcarriers, we adopt channel interpolation using a two-dimensional FFT [12], called a 2D-FFT scheme. In the 2D-FFT scheme, accurate interpolations in the frequency and time domains are achieved only by domain conversion by 2D-FFT and zero sequence insertion. Here, the 2D-FFT scheme is briefly reviewed.

For example, we consider the interpolation of the channel coefficients of Eq. (13). First, the discrete channels of $\hat{H}_{1,i}^{pro.}(k, n)$ are collected as $\bar{H}(k, n)$, given by

$$\begin{aligned} & \bar{H}(k, n) = \hat{H}_{1,i}^{pro.}(N_f k, N_t n) \\ & (k = 0, 1, \dots, N_{pf} - 1), (n = 0, 1, \dots, 2N_{pt} - 1) \end{aligned} \quad (26)$$

where N_{pt} and N_{pf} are the number of reference pilot symbols in the time and the frequency domains, respectively. Next, the window function $W(n)$ is multiplied by $\bar{H}(k, n)$ in the time domain to mitigate the alias effect of the FFT as

$$G(k, n) = \bar{H}(k, n)W(n) \quad (n = 0, 1, \dots, 2N_{pt} - 1) \quad (27)$$

As a window function, the Blackman function is used in this paper as follows:

$$W(n) = 0.423 - 0.498 \cos\left(\frac{\pi n}{N_{pt}}\right) + 0.0792 \cos\left(\frac{2\pi n}{N_{pt}}\right) \quad (n = 0, 1, \dots, 2N_{pt} - 1) \quad (28)$$

Then, $G(k, n)$ is transformed to the transposed domain [13] by 2D-FFT [13], [14], which is described by

$$g(m, l) = \sum_{k=0}^{N_{pf}-1} \left\{ \sum_{n=0}^{2N_{pt}-1} G(k, n) \exp\left(\frac{-j\pi l(n-N_{pt})}{N_{pt}}\right) \cdot \exp\left(\frac{-j2\pi m(k-N_{pf}/2)}{N_{pf}}\right) \right\} \quad (m = -\frac{N_{pf}}{2}, -\frac{N_{pf}}{2} + 1, \dots, \frac{N_{pf}}{2} - 1), \quad (l = -N_{pt}, -N_{pt} + 1, \dots, N_{pt} - 1) \quad (29)$$

where $g(m, l)$ is the transformed function of $G(k, n)$ by 2D-FFT, and m and l are the symbol indices after transformation corresponding to k and n , respectively. Then, the interpolated function $g'(m', l')$ in the transpose domain is generated by the insertion of zero sequences outside of $g(m, l)$, as shown in Eq. (30). This operation corresponds to the interpolation between pilot symbols in the (k, n) -domain.

$$g'(m', l') = \begin{cases} N_{pf}N_{pt}g(m', l'); & -\frac{N_{pf}}{2} \leq m' \leq \frac{N_{pf}}{2} - 1, \\ & -N_{pt} \leq l' \leq N_{pt} - 1 \\ 0; & \text{others} \end{cases} \quad (m' = -\frac{N_{pf}}{2}, -\frac{N_{pf}}{2} + 1, \dots, \frac{N_{pf}}{2} - 1), \quad (l' = -N_{pt}, -N_{pt} + 1, \dots, N_{pt} - 1) \quad (30)$$

where m' and l' are the symbol indices after interpolation, corresponding to m and l , respectively. The interpolated channel $G'(k', n')$ can be obtained by transforming the transpose-domain function $g'(m', l')$ into the frequency-time domain by 2D-IFFT, which is described by

$$G'(k', n') = \frac{1}{N_f N_{pf}} \sum_{m'=-\frac{N_{pf}}{2}}^{(N_f N_{pf})/2} \left\{ \frac{1}{2N_t N_{pt}} \sum_{l'=-N_{pt}}^{N_t N_{pt}-1} g'(m', l') \exp\left(\frac{j\pi l'(n'-N_t N_{pt})}{N_t N_{pt}}\right) \right\} \cdot \exp\left(\frac{-j2\pi m'(k'-N_f N_{pf}/2)}{N_f N_{pf}}\right) \quad (k' = 0, 1, \dots, N_f N_{pf} - 1), \quad (n' = 0, 1, \dots, 2N_t N_{pt} - 1) \quad (31)$$

where k' and n' are the symbol indices after transformation, corresponding to the frequency and the time domains as well as k and n , respectively.

Finally, after dividing the time-domain window function and eliminating the degraded part of both ends due to the alias effect, the estimated channel coefficients $\hat{H}(k', n')$ can be obtained, which are given by

$$\hat{H}(k', n' + N_t N_{pt}/2) = \frac{G'(k', n' + N_t N_{pt}/2)}{W'(n' + N_t N_{pt}/2)} \quad (32)$$

$$(k' = 0, 1, \dots, N_f N_{pf} - 1), (n' = 0, 1, \dots, N_t N_{pt} - 1) \quad W'(n) = 0.423 - 0.498 \cos\left(\frac{\pi n}{N_t N_{pt}}\right) + 0.0792 \cos\left(\frac{2\pi n}{N_t N_{pt}}\right) \quad (n = 0, 1, \dots, 2N_t N_{pt} - 1) \quad (33)$$

Note that N_t , N_f , N_{pt} , and N_{pf} should be powers of two to utilize the 2D-FFT.

Table 1 Calculation complexities of CE with feedback.

	Block	Null	Sparse
Channel estimation	$2N+(3M\log_2 N)/2$	$2N/N_f$	$9N/N_f$
Channel interpolation	$3B$	$3A$	$3A$
Total	$2N+(3M\log_2 N)/2+3B$	$2N/N_f+3A$	$9N/N_f+3A$

Table 2 Calculation complexities of CE without feedback.

	Block	Null	Sparse
Channel estimation	$N+(3M\log_2 N)/2$	N/N_f	$8N/N_f$
Channel interpolation	$2B$	$2A$	$2A$
Total	$N+(3M\log_2 N)/2+2B$	N/N_f+2A	$8N/N_f+2A$

3.6 Complexity Evaluation

The calculation complexities of block-, null-, and sparse-type frames are compared. The number of complex multiplications per frame is counted as the calculation complexity. Tables 1 and 2 show the number of calculations of each scheme with and without feedback, respectively. Here, a two-dimensional FFT is adopted for channel interpolation in all schemes, and the channel estimation based on the proposed correlation is used in the sparse-type frame. Coefficients A and B in the tables are defined in Eqs. (34) and (35), where $A > B$. It is found in Table 1 that the complexity of channel estimation is increased in the block-type frame because the domain transfer by FFT is needed for channel detection. However, the channel interpolation is only in the time domain, and the complexity of that part is reduced. In Table 2, it is found that the calculation complexity is decreased in all types because the estimation is not carried out at the relay node and end nodes jointly conduct channel estimation.

$$A = \frac{N}{N_t N_{pt} N_f N_{pf}} \left(2N_{pt} N_{pf} + N_{pf} N_{pt} \log_2 N_{pf} + N_{pf} N_{pt} \log_2 2N_{pt} + N_t N_{pt} N_f N_{pf} \log_2 N_f N_{pf} + N_t N_{pt} N_f N_{pf} \log_2 2N_t N_{pt} + N_t N_{pt} N_f N_{pf} \right) \quad (34)$$

$$B = \frac{N}{N_t N_{pt}} \left(2N_{pt} + N_{pt} \log_2 2N_{pt} + N_t N_{pt} \log_2 2N_t N_{pt} + N_t N_{pt} \right) \quad (35)$$

4. Numerical Results

In this section, we evaluate the performance of the proposed scheme by computer simulation. The bit error rate (BER) and throughput performances of the channel estimation scheme with/without feedback using block-, null-, or sparse-type frames are evaluated. In the case of a sparse-type frame, the performances with the conventional and the proposed correlation processing are also evaluated.

4.1 Performance of Channel Estimation Scheme with Feedback

The pilot intervals are derived from the system requirements. In this study, we assume the Long Term Evolution (LTE) standard, where the carrier frequency is 3.5 GHz, and the bandwidth is 1.4 MHz. When the maximum velocity of the terminal is 300 km/h, and the maximum multipath delay time is $8T_s$, the optimal pilot intervals become $(N_{f,opt}, N_{t,opt}) = (4, 8)$ from the two-dimensional sampling theorem [15]. Here, T_s is one sample period of the OFDM frame. In what follows, these parameters are used.

4.1.1 Performance Comparison versus E_b/N_0

First, the BER and throughput performances versus E_b/N_0 of the channel estimation scheme with feedback are calculated. Table 3 shows the simulation conditions. The calculation complexity for the conditions in Table 3 is listed in Table 4. The total complexity of the sparse-type frame is the largest and is approximately 24% and 4% higher than that of the block and null types, respectively. A non-systematic convolutional (NSC) code with code rate $R = 1/2$ and con-

Table 3 Simulation conditions.

Frame type	Block	Null	Walsh con.	Walsh pro.
Transmission scheme	OFDM			
Modulation	QPSK			
Number of subcarriers	64			
Packet length [information bits/packet]	512			
Number of GI	10			
Channel	i.i.d. 9-path 3-dB decayed Rayleigh fading			
Normalized delay spread	1.36			
Channel coding	NSC code ($R=1/2$, $K=3$)			
Channel decoding	Hard-decision Viterbi algorithm			
Code length [bits]	2048			
Interleaver	Random			
Interleaver size [bits]	2048			
Channel feedback	Perfect/None			
Time slot 1 pilot period (N_f, N_t)	(1,8)	(2,8)	(4,8)	(4,8)
Time slot 2 pilot period (N'_f, N'_t)	(1,8)	(2,8)	(4,8)	(4,8)
(N_{pf}, N_{pt}) in (26)	(64,4)	(16,4)	(16,4)	(16,4)
Relay scheme	Amplify-and-forward			
Equalization	Zero-forcing criterion			

Table 4 Calculation complexity of CE for the conditions of Table 3.

Channel		Block	Null	Sparse
estimation	with feedback	704	32	144
	without feedback	640	32	256
interpolation	with feedback	1464	2550	2550
	without feedback	928	1696	1696
Total	with feedback	2168	2582	2694
	without feedback	1568	1728	1952

straint length $K = 3$ is adopted for channel coding at the transmitter, and the hard-decision Viterbi algorithm is applied for decoding at the receiver. Furthermore, a random bit interleaver is inserted after the channel encoder output for performance improvement. In Table 3, Walsh con. and Walsh pro. indicate the sparse-type frame using conventional correlation processing and the proposed correlation processing, respectively. Figures 7 and 8 illustrate the BER and throughput performances, respectively, when the normalized Doppler frequency is $f_d T_s = 10^{-4}$ (which corresponds to approximately a 59-km/h node velocity) where f_d is the Doppler frequency. Here, throughput η is defined as follows:

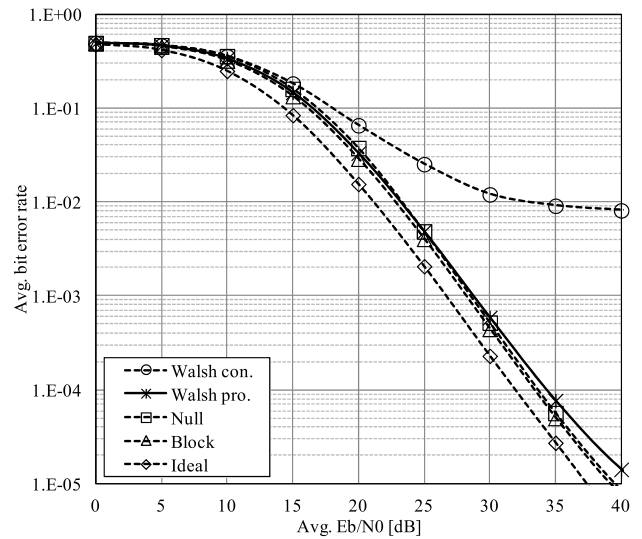


Fig. 7 BER performance versus E_b/N_0 in feedback system at $f_d T_s = 10^{-4}$.

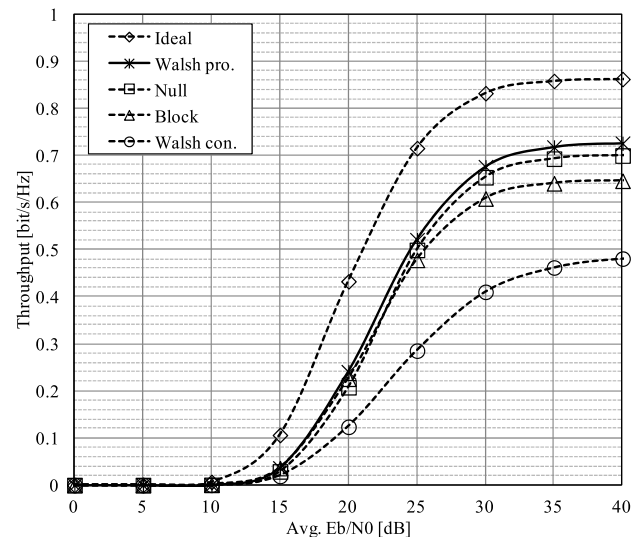


Fig. 8 Throughput performance versus E_b/N_0 in feedback system at $f_d T_s = 10^{-4}$.

$$\eta = MR \frac{N}{N + N_{GI}} \frac{N_f(N_t - F) - 1}{N_t N_f} (1 - PER) \quad (36)$$

where M is the modulation level ($M = 2$), F is the number of OFDM frames for channel feedback, and PER is the packet error rate. In Figs. 7 and 8, ideal indicates the performance with perfect channel state information (CSI). It is assumed that the average E_b/N_0 is the same at both nodes T_1 and T_2 and that the estimated CSI in Time Slot 1 at the relay node R is perfectly fed back to node T_i using one OFDM frame ($F = 1$) [6]. In the figures, the average performance of T_1 and T_2 are plotted.

From the results of Fig. 7, we can see that the proposed scheme has an improved BER performance as compared to conventional correlation processing because the proposed scheme can suppress the interference of time-selective fading. In addition, it is confirmed that the BER of the proposed scheme is not degraded as compared with the block and null types, even though the pilot ratio is lower at $E_b/N_0 \leq 30$ dB. On the other hand, the BER performance of the proposed scheme is slightly degraded at $E_b/N_0 > 30$ dB because of the time-variant interference terms in correlation processing.

This advantage is confirmed by the throughput performance shown in Fig. 8. The throughput of the proposed Walsh scheme is approximately 12% and 4% better than that of the block- and null-type schemes, respectively, at $E_b/N_0 = 40$ dB. As compared with the conventional Walsh scheme that has the same pilot ratio, an improvement of approximately 51% is obtained.

4.1.2 Performance Comparison versus $f_d T_s$

We evaluate the BER and throughput performances of the channel estimation scheme with feedback versus $f_d T_s$. The simulation conditions are the same as those listed in Table 3, and Figs. 9 and 10 show the results at $E_b/N_0 = 30$ dB.

In Fig. 9, all the BER performances are similar at $f_d T_s = 10^{-5}$ (5.9-km/h node velocity), where the time variance of the channel is relatively slow. However, according to the Doppler frequency increase, the BER of the conventional Walsh scheme is degraded from $f_d T_s = 2 \times 10^{-5}$ (12-km/h node velocity) as interferences $\Delta_1^{w.con.}$ and $\Delta_2^{w.con.}$ become large in the correlation processing in Eqs. (11) and (12). On the other hand, the proposed scheme performs well until $f_d T_s = 10^{-4}$ (59-km/h node velocity) because of the robust correlation processing of Eq. (13). As compared to the dense pilot symbol schemes, the BER performance of the proposed scheme is not robust for $f_d T_s$. When comparing the throughput performance, similar characteristics are obtained. Note that the BER is decreased once in proportion to $f_d T_s$ until $f_d T_s = 3 \times 10^{-4}$ (178-km/h node velocity) because the interleaver effectively works and enhances the channel coding performance in this region. That is, in the small $f_d T_s$ region, a long burst error occurs, and the error correcting code does not effectively work even if the interleaver is used. The error is mitigated when $f_d T_s$ is increased.

As shown in Fig. 10, the proposed scheme has the best

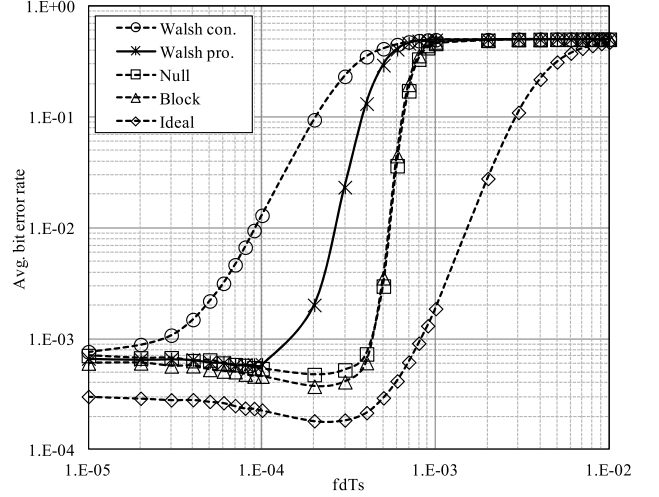


Fig. 9 BER performance versus $f_d T_s$ in feedback system at $E_b/N_0 = 30$ dB.

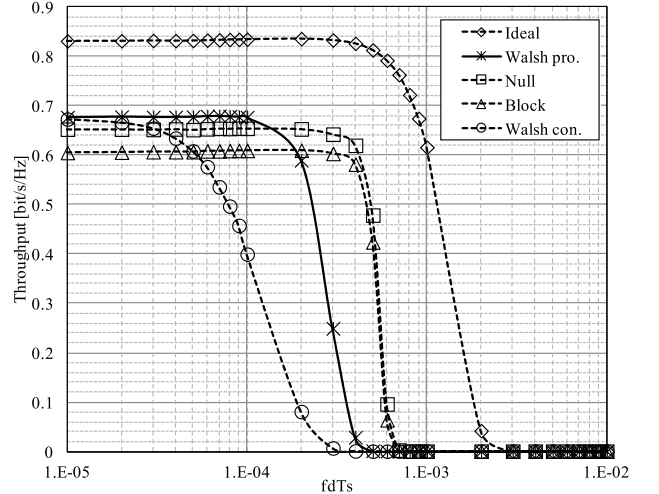


Fig. 10 Throughput performance versus $f_d T_s$ in feedback system at $E_b/N_0 = 30$ dB.

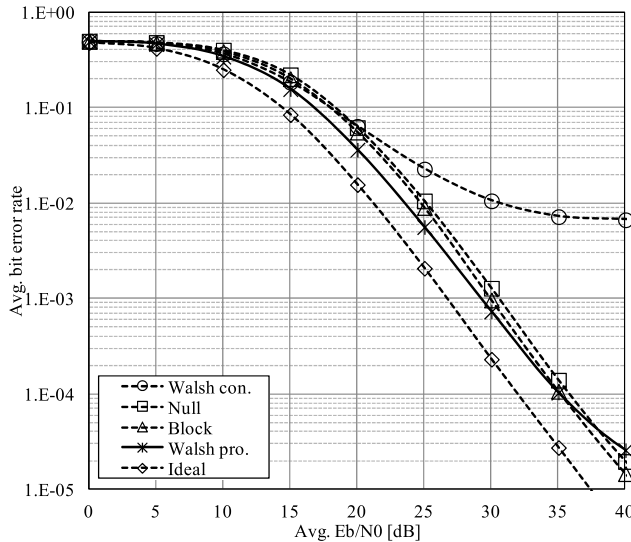
performance until $f_d T_s \leq 1.5 \times 10^{-4}$ (less than 89-km/h node velocity), and the throughput of the proposed scheme at $f_d T_s = 10^{-4}$ (59-km/h node velocity) is approximately 11%, 3%, and 70% better than the block, null, and conventional Walsh schemes, respectively.

4.2 Performance of Channel Estimation Scheme without Feedback

The maximum Doppler frequency and the maximum delay time of the joint channel double for CE without feedback because the relay is simply forwarding the signals and the joint channel becomes a multiplication of both channels in the frequency domain, equivalent to the convolution of them in the time domain. Therefore, the optimal pilot intervals decrease by half in both the time and the frequency domains from Table 3, as shown in Table 5, and we use this coefficient in the following section.

Table 5 Pilot symbol interval for simulation of non-feedback system.

	Block	Null	Walsh con.	Walsh pro.
Time Slot 1 pilot period (N_p , N_t)	(1,4)	(1,4)	(2,4)	(2,4)

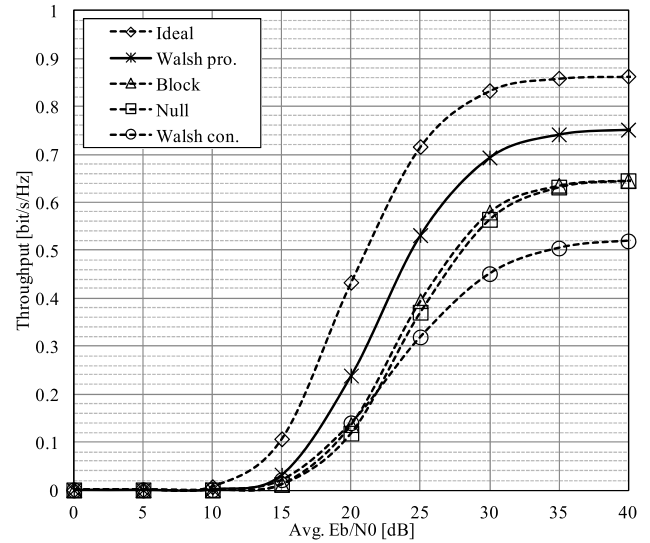
**Fig. 11** BER performance versus E_b/N_0 in non-feedback system at $f_d T_s = 10^{-4}$.

4.2.1 Performance Comparison versus E_b/N_0

In this subsection, we evaluate the BER and throughput performance versus E_b/N_0 of the channel estimation scheme without feedback. The simulation conditions are the same as those listed in Table 3, except for the pilot period, as listed in Table 5. The calculation complexity is also shown in Table 4, which is derived by substituting the parameters of Tables 3 and 5 into Table 2. Similar to the feedback scheme, the complexity of the sparse type is the largest and is approximately 24% and 13% higher than that of the block and null-type schemes, respectively. However, because this scheme can omit the signal processing at the relay node, and the estimation is jointly performed at the end nodes, the complexity is decreased by approximately 28%–30% from the feedback scheme. Figures 11 and 12 show the BER and throughput performances versus E_b/N_0 at $f_d T_s = 10^{-4}$ (59-km/h node velocity), respectively. Here, throughput η is defined by Eq. (36) with $F = 0$.

From the results of Fig. 11, we can see that the proposed scheme has the best performance below $E_b/N_0 = 35$ dB. This is because the arithmetic mean effect of Gaussian noise is emphasized for both Time Slots 1 and 2, as shown in $\Delta_3^{wo.pro.}$ of Eq. (25), and this $\Delta_3^{wo.pro.}$ is mitigated. However, the BER is degraded after $E_b/N_0 = 35$ dB because $\Delta_1^{wo.pro.}$ and $\Delta_2^{wo.pro.}$ become larger than other schemes owing to strong fading selectivity.

Figure 12 shows the throughput performance versus

**Fig. 12** Throughput performance versus E_b/N_0 in non-feedback system at $f_d T_s = 10^{-4}$.

E_b/N_0 . At $E_b/N_0 = 40$ dB, the performance of the proposed scheme is approximately 16%, 17%, and 45% improved for the block, null, and conventional Walsh schemes, respectively, because of the effective channel estimation. Moreover, when compared with Fig. 8, it is found that the performance of the proposed scheme without feedback is approximately 3% better than that with feedback. Because the quantization error and feedback error that occurs in practical cases degrade the estimation performance, it can be said that the estimation scheme without feedback is more effective.

4.2.2 Performance Comparison versus $f_d T_s$

Next, the performance versus Doppler frequency is calculated. The simulation conditions are the same as those listed in Sect. 4.2.1. Figures 13 and 14 show the BER and throughput performances versus $f_d T_s$ at $E_b/N_0 = 30$ dB, respectively. As shown in Fig. 13, the best BER is obtained in the proposed scheme at $f_d T_s \leq 10^{-4}$ (less than 59-km/h node velocity) because of the same reason why this is true for $\Delta_3^{wo.pro.}$ mitigation. However, the BER of the proposed scheme is rapidly degraded at $f_d T_s > 10^{-4}$ (more than 59-km/h node velocity) owing to the interference increase.

From the results of Fig. 14, we can see similar characteristics in Fig. 10. The proposed scheme has the best performance at $f_d T_s \leq 2 \times 10^{-4}$ (less than 118-km/h node velocity). At $f_d T_s = 10^{-4}$ (59-km/h node velocity), the proposed scheme improves the throughput by 19%, 22%, and 56% for the block, null, and conventional Walsh schemes, respectively. As compared to the feedback scheme of Fig. 10, the proposed scheme improves the throughput by 2% at $f_d T_s = 10^{-4}$ (59-km/h node velocity).

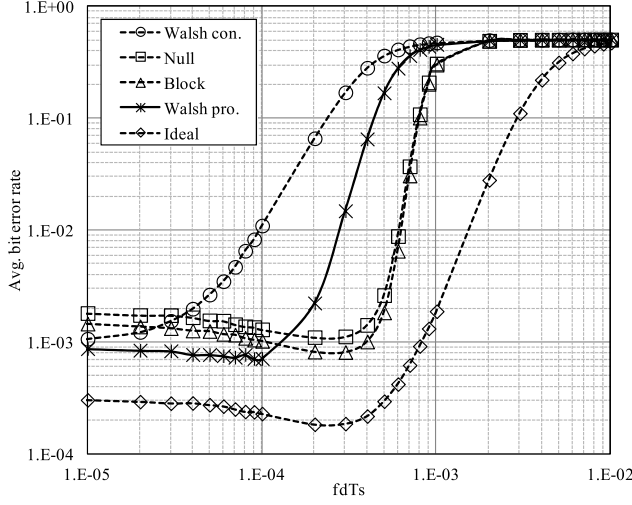


Fig. 13 BER performance versus $f_d T_s$ in non-feedback system at $E_b/N_0 = 30$ dB.

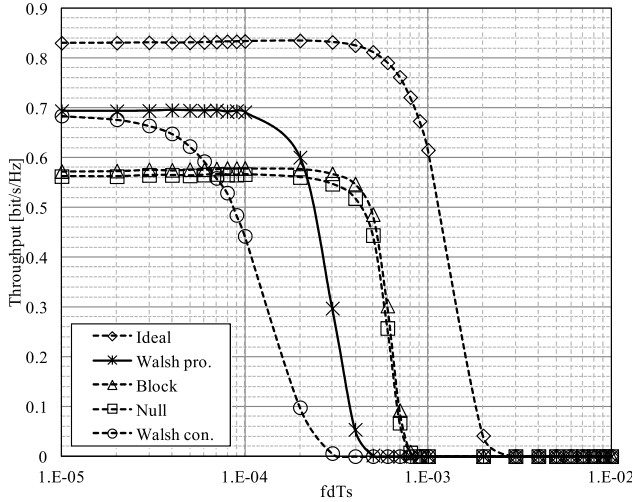


Fig. 14 Throughput performance versus $f_d T_s$ in non-feedback system at $E_b/N_0 = 30$ dB.

4.3 Performance Comparison for Frequency-Selectivity of Channel

Finally, we evaluate the performance for the frequency selectivity of the channel using the configuration of Tables 3 and 5, except for the channel setting. The channel is assumed to be i.i.d. 9-path α -dB decayed Rayleigh fading, and its normalized delay spread is calculated in Table 6. Figure 15 shows the throughput performance versus the normalized delay spread at $E_b/N_0 = 30$ dB and $f_d T_s = 10^{-4}$ (59-km/h node velocity). It is found that the proposed schemes have the best throughput among the four schemes without the ideal case. This is achieved by the rate efficiency of the sparse pilots and the accurate interpolation of the 2D-FFT. In addition, the performance is improved as the delay spread increases. In strong frequency-selective fading,

Table 6 Relationship between attenuation parameter α and normalized delay spread τ_{rms}/T_s .

α [dB]	0	1	2	3	4	5
τ_{rms}/T_s	2.58	2.33	1.82	1.36	1.04	0.821
α [dB]	6	7	8	9	10	
τ_{rms}/T_s	0.669	0.558	0.473	0.406	0.351	

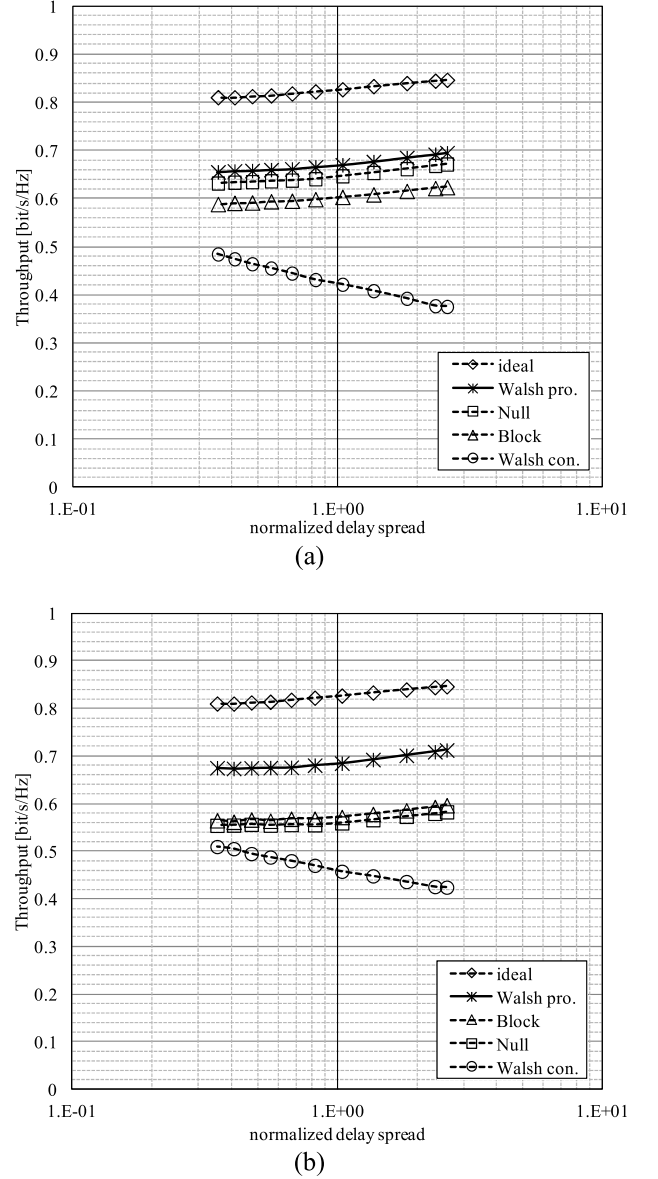


Fig. 15 Throughput performance versus delay spread at $E_b/N_0 = 30$ dB; (a) with feedback, (b) without feedback.

the burst attenuation of the channel coefficients in the frequency domain occurs less, and the channel coding effectively works in those channels.

5. Conclusion

In this paper, we proposed a channel estimation scheme

for bi-directional relay systems with ANC. In the proposed scheme, the bi-directional overlapped channels can be separated by utilizing Walsh codes as pilot symbols at the transmitter, and the improved correlation processing in the receiver can generate an accurate and robust fading estimation in terms of the time- and frequency selectivity of fading. In addition, the proposed scheme can utilize the sparse pilot symbols and increase the rate efficiency. From the numerical results, it has been confirmed that the proposed channel estimation scheme shows better performance under relatively slow fading environments. In particular, the proposed scheme with and without feedback has the best performance at $f_d T_s \leq 1.5 \times 10^{-4}$ (less than 89-km/h node velocity) and $f_d T_s \leq 2 \times 10^{-4}$ (less than 118-km/h node velocity), respectively. When the proposed scheme without feedback is compared with that with feedback, the BER performance is slightly degraded because of the joint channel characteristics. However, it is found that the proposed scheme without feedback can omit the feedback link and has the better throughput performance. In conclusion, the proposed scheme without feedback can generate accurate channel estimation and good performance when $f_d T_s$ is relatively small.

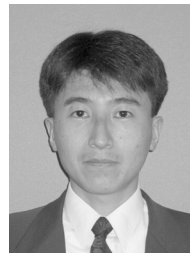
The configuration of a practical feedback link is an additional topic in this paper and will be studied in the future.

References

- [1] S. Zhang, S. Liew, and P. Lam, "Physical layer network coding," ACM MobiCom, Sept. 2006.
- [2] S. Katti, H. Rahul, D. Katabi, W.H. M. Medard, and J. Crowcroft, "XORs in the air: Practical wireless network coding," SIGCOMM, 2006.
- [3] S. Katti, S. Gollakota, and D. Katabi, "Embracing wireless interference: Analog network coding," SIGCOMM, 2007.
- [4] H. Gacanin and F. Adachi, "Broadband analog network coding," IEEE Trans. Wireless Commun., vol.9, no.5, pp.1577–1583, May 2010.
- [5] H. Gacanin, T. Sjodin, and F. Adachi, "On channel estimation for analog network coding in a frequency-selective fading channel," EURASIP J. Wireless Communications and Networking, Article ID 980430, doi:10.1155/2011/980430, 2011.
- [6] I. Prodan, T. Obara, F. Adachi, and H. Gacanin, "Performance of pilot-assisted channel estimation without feedback for broadband ANC systems using OFDM access," EURASIP J. Wireless Communications and Networking, doi:10.1186/1687-1499-2012-315, 2012.
- [7] Y. Koshimizu and E. Okamoto, "An effective channel estimation scheme for bi-directional two-timeslot OFDM relay transmission using analog network coding," IEEE VTC-Spring, May 2012.
- [8] Y. Koshimizu and E. Okamoto, "An efficient channel estimation scheme without feedback from relay in bi-directional two-timeslot OFDM relay systems," IEICE Technical Report, RCS2012-172, Nov. 2012.
- [9] H. Joen, H. Song, and E. Serpedin, "Walsh coded training signal aided time domain channel estimation for MIMO-OFDM systems," IEEE Trans. Commun., vol.56, no.9, pp.1430–1433, Sept. 2008.
- [10] H. Furuta and T. Ikeda, "A study on estimating channel state information for a MIMO-OFDM studio-camera radio system," IEICE Technical Report, RCS2003-222, 2003.
- [11] J. Siew, R.J. Piechocki, A. Nix, and S. Armour, "A channel estimation method for MIMO-OFDM systems," Proc. London Communications Symp., Sept. 2002.
- [12] D. Motokawa, H. Hayashi, E. Okamoto, and Y. Iwanami, "A study on sparse pilot symbol for single carrier-frequency domain equalization," Proc. Int'l. Sym. Wireless Personal Multimedia Commun. (WPMC), Sept. 2009.
- [13] M.K. Ozdemir and H. Arslan, "Channel estimation for wireless OFDM systems," IEEE Commun. Surveys and Tutorials, vol.9, no.2, pp.18–48, 2007.
- [14] Y. Zhao and A. Huang, "A novel channel estimation method for OFDM mobile communication systems based on pilot signals and transform-domain processing," Proc. IEEE 47th Vehicular Technology Conf., vol.3, pp.2089–2093, May 1997.
- [15] P. Hoeher, S. Kaiser, and P. Robertson, "Two-dimensional pilot-symbol-aided channel estimation by Wiener filtering," Proc. 1997 IEEE Int. Conf. Acoustics, Speech, and Signal Processing, pp.1845–1848, April 1997.



Yuta Koshimizu received the B.E. and M.S. degrees in Electrical Engineering from Nagoya Institute of Technology in 2011 and 2013, respectively. His research interests were in the areas of wireless communication and channel estimation.



Eiji Okamoto received the B.E., M.S., and Ph.D. degrees in Electrical Engineering from Kyoto University in 1993, 1995, and 2003, respectively. In 1995 he joined the Communications Research Laboratory (CRL), Japan. Currently, he is an associate professor at Nagoya Institute of Technology. In 2004 he was a guest researcher at Simon Fraser University. He received the Young Researchers' Award in 1999, Communications Society: Distinguished Contributions Award in 2005, 2007, and 2010 from IEICE, and the FUNAI Information Technology Award for Young Researchers in 2008. He also received the Excellent Paper Award in International Conference on Information Networking (ICOIN) and the research award from technical committee on satellite communications in 2012. His current research interests are in the areas of wireless technologies, satellite communication, and mobile communication systems. He is a member of IEEE.